Algal Magnetic Nickel Oxide Nanocatalyst in Accelerated Synthesis of Pyridopyrimidine Derivatives

Foad Buazar (fb@kmsu.ac.ir)
Khorramshahr University of Marine Science and Technology
Javad Moavi
Khorramshahr University of Marine Science and Technology
Mohammad Hosein Sayahi
Payame Noor University

Research Article

Keywords: nickel oxide nanoparticles, nanocatalyst, marine macroalgae extract, green synthesis, reusability

Posted Date: November 30th, 2020

DOI: https://doi.org/10.21203/rs.3.rs-113388/v1

Version of Record: A version of this preprint was published at Scientific Reports on March 18th, 2021. See the published version at https://doi.org/10.1038/s41598-021-85832-z.

Abstract

This research presents a novel biological route for the biosynthesis of nickel oxide nanoparticles (NiO NPs) using marine macroalgae extract as a reducing and coating agent under optimized synthesis conditions. XRD and TEM analyses revealed that phytosynthesized NiO NPs are crystalline in nature with a spherical shape having a mean particle size of 11±1 nm. It is found that biogenic NiO NPs is a highly efficient catalyst for benign one-pot preparation of pyridopyrimidine derivatives using aqueous reaction conditions. This environmentally friendly procedure takes considerable advantages of shorter reaction times, excellent product yields (up to 96%), magnetically reusable nanocatalyst (7 runs), low catalyst loadings, and free toxic chemical reagents.

Introduction

In recent years, the marine realm contribution to the production of versatile nanoparticles has undergone significant growth across international research communities since its economic, rapid, and environmental procedure render a viable template for the biosynthetic route [1,2]. Marine organisms (e.g. algae, yeast, bacteria, fungal species) owing to possessing a broad variety of electron-rich phytochemicals such as polyphenols, carbohydrates, polyols, alkaloids, proteins, polysaccharides, peptides, and amino acids, establish a sing-step and comprehensive platform for the simultaneous reduction of metal cations and stabilization of biofabricated nanoparticles [3]. In contrast to commonly employed physical and chemical approaches, the sheer growing demand for uses of green processes presumably due to environmental compatibility, simplicity, and the absence of detrimental chemical reagents [4]. Algae are highly diversified naturally occurring microbes and inhabitants of various aquatic environments such as marine- and fresh-water. These microorganisms are commercially and biologically of great importance since they contain valuable phytoconstituents that address the global market needs through virtual engagement in commercial products, for instance, cosmetics, biofuel, and drugs. In the aspect of biosynthesis, marine algae are known as “bionanofactory”, and hence, different nanoscale materials including alumina, zinc oxide, gold, have been synthesized through miscellaneous algae as a competent green synthesis method [5-7].

Catalyst is a focal point in enormous chemical reactions and has been gaining a surge of popularity particularly in academic and industrial synthetic reactions areas over the past decades. Interestingly, convergence between nanoscience and chemistry led to the advent of nanocatalysts in which as a result of immense surface areas and expansive catalytic capabilities, have attracted great attention of many organic chemists in a myriad of catalyzed-reactions [8,9]. Apart from using a trace amount of catalyst, nanocatalysis processes dramatically enhance the contact between the active component of the catalyst and reactants and therefore increase the rate and yield of chemical reactions [10]. A vast majority of the heterogeneous and homogenous catalysts are pertinent to transition metal nanoparticles due to their unprecedented physicochemical properties. Among these tremendous efforts, nickel oxide nanoparticles have been developed as an efficient catalyst in chemical synthesis of a wide range of valuable organic

compounds such as spiro and condensed indole derivatives [11], aromatic heterocycle [12], 5-substituted 1h-tetrazoles [13], quinolines [14], and spirooxindoles [15]. There are a variety of green methods that have been addressed the construction of the nickel oxide nanoparticles (NiO NPs), mostly relied on plant-assisted bioreduction strategy [16-18].

Pyridopyrimidines and their fused heterocycles derivatives are of paramount importance due to their significant biological and pharmacological activities. Moreover, owing to the involvement of pyridopyrimidine skeleton in some essential medicinal drugs, they hold great promise in the area of pharmaceutical science. Compounds possessing the pyrido[3,2-d]pyrimidines scaffold demonstrate a broad spectrum of biological activities such as antiviral [19,20], antimicrobial [21], antihypertensive, anti-tumor [22], antihistaminic [23], antimalarial, potent inhibitor of protein kinases[24], treatment of diarrhea [25], anti-inflammatory and analgesic activity [26], along with other medicinal applications (scheme 1) [27]. Due to their large variety of characteristics, there has been a growing demand in the design and production of pyridopyrimidine nucleus derivatives in particular those derived from proactive biological procedures.

In this study, proceeding our interest toward green nanoparticle synthesis and application[28], we report a novel biosynthetic method to produce NiO NPs through electron-rich marine algae extract by optimizing these reaction conditions. Afterward, the catalytic efficiency of marine-assisted NiO NPs was explored in the eco-friendly synthesis of pyridopyrimidine derivatives by one-pot three-component elaborated in green conditions. The entire synthetic reaction was performed in water as a highly desirable solvent where increases the environmental impact and economical perspective of the designed protocol[29]. Based on the literature survey, this is the new report on the use of marine algae-assisted NiO NPs as a heterogenetic catalyst in organic synthesis of a library of pyridopyrimidine heterocyclic compounds through newly four-component condensation.

Results And Discussion

UV-visible spectroscopy analysis

The initial evidence of NiO NPs formation was revealed when the solution color changed from brown to dark green. Correspondingly, the UV-vis spectrum demonstrated a characteristic absorbance peak at 330 nm indicating biofabrication of NiO NPs in the extract of marine algae biomass (Figure 1a,b). The completion of the reaction was monitored in UV visible spectra as a function of time (5 min, 10 min, 20 min, 30 min, and 1h). The results show that the apex of the absorption peak intensity was observed at 30 min indicating the reduction of nickel ions to zero valance metallic nickel atom. Moreover, no sensible changes have been observed in peak position when the sample stored up to 6 months in the laboratory, indicating high stability of bioproduced NiO NPs in aqueous green media. Previous studies reported the optical absorption peak of biological NiO NPs in the range of 330-350 nm using green synthesis methods [17,18,30] which are in good agreement with our results.

XRD analysis

The phase structure of marine algae-mediated NiO NPs is further scrutinized by the X-ray diffraction technique. The XRD results show that the face center cubic (FCC) facets of green NiO NPs crystalline lattice is attributed to prominent diffraction peaks and miller indexes (hkl) at 37.45°(111), 43.15°(200), 62.77°(220), 75.34°(311) and 79.64°(222), respectively (Figure 2). Owing to the nonappearance of impurity peaks, the biofabricated nanoparticles were highly pure in nature. In addition, our obtained data are well-matched with JCPDS No: 98-009-0610, showing similar results to literature reports concerning biosynthesized NiO NPs [31-33]. Based on the high intensity of Bragg peak at 43.15°(200), the calculated median crystallite size of NiO NPs was 8 nm using Debye–Scherrer's formula.

TEM characterization

The particle size and morphology and of NiO NPs were determined through the TEM analysis. TEM images confirmed that the vast majority of the particles were particles relatively non-spherical in shape, however, they appear in uniform and smooth morphology in the green synthesis platform as highlighted in Figure 3a. It can be noted that some regions of the sample appear darker in TEM image of bioprepared NiO NPs perhaps as a result of variation in thickness or high mass density of particles. Furthermore, the TEM image assay exhibited that biogenic NiO NPs possess a median diameter of 11 ±1 nm obtained through counting 250 particles as performed by ImageJ software [34]. EDX analysis confirmed the major components of the sample with nickel and oxygen atoms indicating the purity of biogenic Ni NPs (Figure 3b). The Au element detected in the EDX analysis was resulted from the gold-coated grid used for SEM specimen preparation.

FTIR analysis

FTIR spectroscopy is a powerful tool to determine organic constituents qualitatively in seaweeds and plants [5]. The recorded spectrum presents a wide variety of prominent functional groups on the surface of biological NiO NPs as depicted in Figure 4. The estimation of the class of organic moieties in the seaweeds is of great value since it would elucidate their role in the reduction and capping of freshly produced nanoparticles in the green medium. The strong wide band at 3411 cm^{-1} is characteristic of electron-rich N—H and O—H stretching vibrations, presenting amino acid and hydroxyl groups of polysaccharides. The weak C-H stretching mode at 2945 cm^{-1} is attributed to the CH_2 and CH_3 groups of aliphatic compounds. The characteristic absorption peak around 1640 cm^{-1} is on account of the presence of C=O, pertaining to ester groups. The C=C absorption band representative of the lignin is observed at 1545 cm^{-1}. The absorption band centered at 1322 cm^{-1} indicates S=O stretching of sulfated polysaccharide entity. Doublet symmetric C—O vibration peaks appeared at 1030 and 1193 cm^{-1} may belong to ethers and glycosidic of carbohydrates. The advent of strong characteristic vibrations at 525 and 685 cm^{-1} indicate Ni-O bonds in the fingerprint region [17,31]. These results show the interaction of algal electron donor biomolecules with nickel cations maybe lead to the reduction as well as coating as-prepared NiO NPs. Apparently phytochemical presence in plant or microorganism extracts especially

oxygen-contain biomolecules are acted through an oxidation-reduction mechanism, affording an appropriate reaction medium to generate eco-friendly nanomaterials [35].

VSM properties of NiO NPs

The vibrating sample magnetometer (VSM) analyzer was used to measure the probable magnetic amount of biologically formed NiO NPs. Figure 5 illustrates the magnetization M curve of green NiO NPs, after annealing, at fields of −10 and +10 Oersted. The M and H lines are not intersected in the entire curve indicating that coercivity (H_c) and remanent magnetization (M_r) were naught. As a result, algal NiO NPs could deem as superparamagnetic material. The saturation magnetization (M_s) is the maximum value of magnetic induction and is size-dependent in which crystal lattice defects, inferior agglomeration state of the particles, size smallness, and higher surface-to-volume ratio would induce higher magnetic properties. Based on the VSM graph, Ms value of biogenic NiO NPs was measured as 0.198 emu/g which displays superior magnetization rather than reported plant-based NiO NPs [36]. It is well known that bulk grain-sized nickel oxide reveals antiferromagnetic susceptibility at room temperature [37], whereas superparamagnetism is evidently a function of particle size [38] for nanoparticles particularly below 20 nm as indicated for green NiO NPs.

Catalytic performance of biological NiO NPs

In order to determine the optimal conditions of the reaction, we investigate the different amount of NiO catalyst required for the environmentally friendly synthesis of pyridopyrimidine derivatives using a straightforward four-component reaction approach of thiobarbituric acid **1**, 4-hydroxy coumarin **2**, aldehyde **3**, and ammonium acetate **4** as model substrates in water solvent condition (scheme 2). It is found that the best yield of products (95%) was achieved when the molar concentration of nanoparticles reached 5% (Table 1). It is noted that neither yield nor rate was revealed significant improvement by loading a larger amount of NiO nanocatalyst as illustrated in Table 1.

Table 1 Effect of catalytic amount of green NiO NPs in the aqueous synthesis of **5g**

Entry	Catalytic conc. (mol%)	Time (min)	Yield (%)
1	2	40	75
2	5	40	95
3	10	40	95
4	15	40	90
5	20	40	85

To assess the effectiveness of the catalytic activity of generated NiO NPs, a test reaction was explored in presence of various catalysts with respect to the reaction time of choice in an aqueous medium (Table 2). Generally, in the absence of a catalyst at a consistent temperature of 40 °C only offered trace yield of the expected products (entry 6). The results showed that the highest yield of products was obtained when biogenic NiO NPs contributed to the model reaction (entry 4). Moreover, introducing chemical-produced NiO NPs increases the resultants yield rather than conventional catalysts (entries 1,3,5) in a shorter time whereas it produced lower yield rather than algal NiO NPs (entry 2). It is found that the occurrence of plant-derived phytochemical constituents on the surface of bio-assisted nanoparticles during the synthesis process, would tune the distinctive parameters of decorated nanomaterials such as morphology and particle-size distribution which in turn improve their catalytic properties rather than plain traditional catalysts [6]. As a result, the designed algal NiO NPs-catalyzed organic synthesis takes major advantages including excellent yields, short time, low cost, simplicity, green chemical reaction condition, and environmental sustainability.

Entry	Catalyst	Time (h)	Yield (%)
1	bulk Ni oxide	4	61
2	commercial NiO NPs	1	80
3	acetic acid	2	50
4	biogenic NiO NPs	40	95
5	HCl	1.5	30
6	neat	24	trace

Table 2 Comparison the efficacy of different catalysts in **5g** product preparation.

Recyclability of the nanocatalyst

The recycling of the catalyst is a pivotal point in the procedure of organic synthesis. In order to probe the reusability of biological magnetic NiO NPs; it was isolated from the reaction medium via an external magnet and washed several times with plenty of ethanol and water to achieve an unpolluted catalyst. It is found that no noticeable deterioration in the catalytic performance of algal NiO NPs was detected when it subjected to successive catalytic runs (up to seven) as depicted in Figure 6. Therefore, the desired pyridopyrimidine derivatives could furnish in the proficient yield in the presence of bioprepared NiO NPs.

Scope and limits of biogenic NiO NPs efficiency

The generality of catalytic efficiency of NiO NPs was investigated using a library of miscellaneous functionalized organic aldehydes moieties under the optimized reaction conditions. Regardless of induced substituents, the produced pyridopyrimidine derivatives furnished in high product yields with appreciable purity, confirming the profound effect of green NiO NPs. Nevertheless, the variation of

electron-donating and electron-withdrawing groups relatively change the yield of products. Moreover, the highest increase in the rate and product yield was acquired when the NO_2 group was replaced at the para-position of aryl aldehyde producing the target product (**5g**) with a yield of 96% (Table 3, entry 7, Fig. S2).

Table 3 NiO NPs-catalyzed the synthesis of pyridopyrimidine derivatives[a]

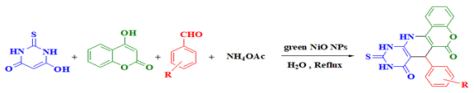

Entry[a]	R	Product		Yield (%)[b]	Melting point (lit.) °C
1	H	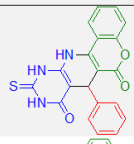	**5a**	88	235-237 (236-238)[39]
2	2-Cl	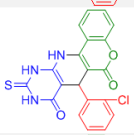	**5b**	92	215-217 (218-220)[39]
3	3-Cl	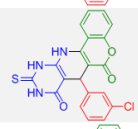	**5c**	90	220-222 (219-220)[39]
4	4-Cl	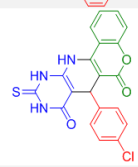	**5d**	94	246-248 (244-246)[39]
5	2,4-DiCl	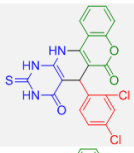	**5e**	85	227-229
6	2-NO_2	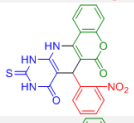	**5f**	90	236-238
7	4-NO_2	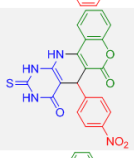	**5g**	96	240-242
8	3-OCH_3	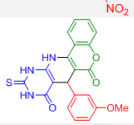	**5h**	88	221-223
9	4-CN	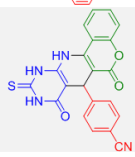	**5i**	92	245-247
10	4-Br	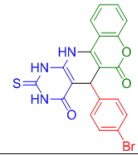	**5j**	90	233-235

[a]Reaction conditions: 4-hydroxy coumarin (1 mmol), ammonium acetate (1 mmol), thiobarbituric acid (1 mmol), aromatic aldehyde (1 mmol), and NiO NPs (5% mol).
[b]Isolated yield

Pyridopyrimidines synthesis mechanism

According to the literature, a possible mechanism is proposed in scheme 3 showing the pathway of catalyzed sequential multicomponent reactions. In the initial step, the enolic form of thiobarbituric acid (**1**) reacts with the catalyst-activated carbonyl of aryl aldehyde (**3**) through Knoevenagel condensation, to generate the α,β-unsaturated compound **6** followed by a dehydration reaction. In the next step, a reaction between 4-hydroxy coumarin (**2**) and in situ produced ammonia from ammonium acetate (**4**) is proposed to give 4-amino coumarin (**5**) at 100 °C. Then, via Michael addition of enamine (**5**) to an alpha, beta-unsaturated carbonyl acceptor of **6**, the intermediate **7** is formed. In the final step, the intramolecular ring cyclization occurs with an amino group attack on the carbonyl group with aid of NiO catalyst after the loss of H_2O. As a result, the desired products **5a-l** are promoted within an aqueous medium at the appropriate time (Scheme 3). Apparently, introducing algal NiO NPs to the designed reaction would simultaneously boost the electrophilic character of the reactants and facilitate the attack of nucleophile groups owing to its acidic character. In addition, Lewis acid NiO nanocatalyst increases the generated intermediate stability and enhances the reactivity of organic materials as well [40,41].

Conclusion

We have demonstrated an efficient synthetic approach for biosynthesis of nickel oxide nanoparticles using marine red algae extract as a novel natural source in the absence of hazardous reagents. It is found that algae-derived phytochemicals are effectively involved in bioreduction and coating as-prepared nanoparticles in benign conditions. The formation of NiO NPs was confirmed by using UV-vis, FTIR, XRD, TEM, and EDX techniques. Our findings show that algal NiO NPs function as a highly robust catalyst for four-component one-pot facile preparation of pyridopyrimidine derivatives in water as a green solvent. The easy magnetic separation and high reusability of up to seven consecutive cycles indicated the substantial catalytic activity of green NiO NPs. The sustainability, economic feasibility, and environmental compatibility of the proposed procedure provide a broad range of uses in processing and green synthesis of organic compounds.

Materials And Methods

All utilized chemicals in this study were obtained from Merck and used as received without any further purification. The formation of biofabricated NiO NPs was scrutinized using a UV-vis (Analytic Jena-Germany) spectrophotometer in the spectral range of 200–700 nm. To detect content variations of the functional groups, the FTIR spectra of the materials were recorded on Nicolet MAGNA-IR 550 spectrometer (Madison, WI, USA) by a KBr pellet. X-ray powder diffraction (XRD) diffractometer (Cu Ka, radiation, λ=1.5405Å) was run at a scanning speed of 2/min from 10 to 80 (2θ), examining the crystal structure of nanoparticles. To explore the magnetic properties of the nanoparticles, a vibrating sample magnetometer. (VSM, model BHV-55, Riken, Japan) the experiment was operated with a magnetic field up to 10 kOe. The morphology and particle size were obtained via transmission electron microscopy (TEM) operating with a Leo 912 AB at an accelerating voltage of 200 kV. For organic product characterization, melting points were gauged using the electrothermal IA9200 apparatus. Compositional

analysis of the sample was carried out by X-ray energy dispersive spectroscopy (EDX). The progress of the reactions and assessment of the purity of the substrate was followed with TLC using silica gel SILG/UV 254 and 365 plates. The specimens of red marine algae were gathered from the intertidal zone in coastal areas of Bushehr province, Iran, during low tide.

Preparation of marine algae extract

In order to obtain a proper extract, in a 100 mL beaker 2 g of washed and under shade-dried powdered algae was soaked in 20 mL of distilled water under stirring at 180 rpm using a magnetic stirrer for 1 h then sonicated at 70 °C for 25 min. Further, the mixture was boiled for 10 min then cooled to room temperature and filtered through Whatman filter paper Grade No 1 (pore size: 11 µm). Eventually, the resultant crude extract was stored in an air-tight container and placed in the refrigerator for additional processing.

Phyto-synthesis of NiO NPs

To synthesize nickel oxide nanoparticles, 10 mL of an aqueous solution of $NiCl_2{\cdot}6H_2O$ (0.01 M) was added to 90 mL of marine red algae extract. The reaction mixture containing red algae extract and nickel chloride hydrate solution was magnetically stirred at 800 rpm for 30 min at 60 °C to attain a homogeneous solution. After cooling down to room temperature, the purification of the resulting solution was fulfilled through continuous centrifugation at 12000 rpm for 20 min with distilled water and ethanol to eliminate undesirable impurities followed by decanting. The obtained precipitate specimen was annealed at 550 °C for 90 min.

Synthesis of pyridopyrimidines derivatives over NiO NPs catalyst

A mixture of ammonium acetate (**4**, 1 mmol) and 4-hydroxy coumarin (**2**,1 mmol) was refluxed in water (15 ml) for 30 min. Then, thiobarbituric acid (**1**,1 mmol), and aromatic aldehyde (**3**,1 mmol) in the presence of green NiO NPs (5 mol %) as a heterogeneous catalyst were added and the reaction was stirred for further 30 min (Scheme 2). Upon completion of the reaction as monitored by TLC, the reaction solution was allowed to cool down to room temperature, subsequently, the 50 H_2O was added to precipitate, filtered out and dried. The solid magnetic nanocatalyst was then separated by centrifugation and an external magnetic force, washed with 10 mL of pure ethanol, dried at 80 °C overnight, and reused. In order to afford uncontaminated products, the precipitate was boiled in 15 mL of EtOH for 5 min, and the final crystalline products were characterized using FTIR, elemental analysis, ^{1}H and ^{13}C NMR spectroscopic techniques (Figs. S1-S4, see supplementary).

Declarations

Contributions

J. Moavi conducted experiments associated with nickel oxide biosynthesis and their spectroscopic characterization. F. Buazar supervised the study, designed the research framework, and carried out the data analysis. M.H. Sayahi participated in setting up an experiment of synthesis of pyridopyrimidines derivatives over NiO NPs catalyst and analyzing results. The final manuscript has been written and edited by F.Buazar with contributions from all coauthors.

Competing interests

The authors declare no competing interests.

References

1 Patil, M. P. & Kim, G.-D. Marine microorganisms for synthesis of metallic nanoparticles and their biomedical applications. *Colloids and Surfaces B: Biointerfaces* **172**, 487-495 (2018).

2 Bajpai, V. K. *et al.* Developments of cyanobacteria for nano-marine drugs: relevance of nanoformulations in cancer therapies. *Marine drugs* **16**, 179 (2018).

3 Khalafi, T., Buazar, F. & Ghanemi, K. Phycosynthesis and enhanced photocatalytic activity of zinc oxide nanoparticles toward organosulfur pollutants. *Scientific reports* **9**, 1-10 (2019).

4 Mohanta, D. & Ahmaruzzaman, M. Addressing Nanotoxicity: Green Nanotechnology for a Sustainable Future. *The ELSI Handbook of Nanotechnology: Risk, Safety, ELSI and Commercialization*, 103-112 (2020).

5 Koopi, H. & Buazar, F. A novel one-pot biosynthesis of pure alpha aluminum oxide nanoparticles using the macroalgae Sargassum ilicifolium: A green marine approach. *Ceramics International* **44**, 8940-8945 (2018).

6 Sepahvand, M., Buazar, F. & Sayahi, M. H. Novel marine-based gold nanocatalyst in solvent-free synthesis of polyhydroquinoline derivatives: Green and sustainable protocol. *Applied Organometallic Chemistry* **34**, 1-11 (2020).

7 LewisOscar, F. *et al.* Algal nanoparticles: synthesis and biotechnological potentials. *Algae–Organisms for Imminent Biotechnology* **7**, 157-182 (2016).

8 Kalidindi, S. B. & Jagirdar, B. R. Nanocatalysis and prospects of green chemistry. *ChemSusChem* **5**, 65-75 (2012).

9 Polshettiwar, V. & Varma, R. S. Green chemistry by nano-catalysis. *Green Chemistry* **12**, 743-754 (2010).

10 Zeng, H. C. Integrated nanocatalysts. *Accounts of Chemical Research* **46**, 226-235 (2013).

11 Sachdeva, H., Dwivedi, D., Bhattacharjee, R., Khaturia, S. & Saroj, R. NiO nanoparticles: an efficient catalyst for the multicomponent one-pot synthesis of novel spiro and condensed indole derivatives. *Journal of Chemistry***2013**, 1-10 (2013).

12 Kaur, N. Nickel catalysis: six membered heterocycle syntheses. *Synthetic Communications***49**, 1103-1133 (2019).

13 Halder, M. *et al.* Sustainable Generation of Ni (OH) 2 Nanoparticles for the Green Synthesis of 5-Substituted 1 H-Tetrazoles: A Competent Turn on Fluorescence Sensing of H2O2. *ACS omega***3**, 8169-8180 (2018).

14 Reddy, B. P., Iniyavan, P., Sarveswari, S. & Vijayakumar, V. Nickel oxide nanoparticles catalyzed synthesis of poly-substituted quinolines via Friedlander hetero-annulation reaction. *Chinese Chemical Letters***25**, 1595-1600 (2014).

15 Nasseri, M. A., Kamali, F. & Zakerinasab, B. Catalytic activity of reusable nickel oxide nanoparticles in the synthesis of spirooxindoles. *RSC Advances***5**, 26517-26520 (2015).

16 Imran Din, M. & Rani, A. Recent advances in the synthesis and stabilization of nickel and nickel oxide nanoparticles: a green adeptness. *International journal of analytical chemistry***2016** (2016).

17 Iqbal, J. *et al.* Phytogenic Synthesis of Nickel Oxide Nanoparticles (NiO) Using Fresh Leaves Extract of Rhamnus triquetra (Wall.) and Investigation of Its Multiple In Vitro Biological Potentials. *Biomedicines***8**, 117 (2020).

18 Haider, A. *et al.* Green synthesized phytochemically (Zingiber officinale and Allium sativum) reduced nickel oxide nanoparticles confirmed bactericidal and catalytic potential. *Nanoscale Research Letters***15**, 1-11 (2020).

19 DeGoey, D. A. *et al.* Discovery of pyrido [2, 3-d] pyrimidine-based inhibitors of HCV NS5A. *Bioorganic & medicinal chemistry letters***23**, 3627-3630 (2013).

20 Nasr, M. N. & Gineinah, M. M. Pyrido [2, 3-d] pyrimidines and Pyrimido [5', 4': 5, 6] pyrido [2, 3-d] pyrimidines as New Antiviral Agents: Synthesis and Biological Activity. *Archiv der Pharmazie: An International Journal Pharmaceutical and Medicinal Chemistry***335**, 289-295 (2002).

21 Tandel, H. T. & Patel, S. K. Efficient procedure with new fused pyrido [2, 3-d] pyrimidine derivatives as potent antimicrobial agents. (2020).

22 Colbry, N. L., Elslager, E. F. & Werbel, L. M. Folate antagonists. 21. Synthesis and antimalarial properties of 2, 4-diamino-6-(benzylamino) pyrido [3, 2-d] pyrimidines. *Journal of medicinal chemistry***28**, 248-252 (1985).

23 Mohire, P. P. *et al.* An Expedient Four Component Synthesis of Substituted Pyrido-Pyrimidine Heterocycles in Glycerol: Proline Based Low Transition Temperature Mixture and Their Antioxidant Activity with Molecular Docking Studies. *Polycyclic Aromatic Compounds*, 1-19 (2020).

24 D'agostino, L. A. *et al.* Substituted pyrido [2, 3-d] pyrimidines as inhibitors of protein kinases. USA patent (2020).

25 Kots, A. Y. *et al.* Pyridopyrimidine derivatives as inhibitors of cyclic nucleotide synthesis: application for treatment of diarrhea. *Proceedings of the National Academy of Sciences***105**, 8440-8445 (2008).

26 Dasari, S. R., Tondepu, S., Vadali, L. R. & Seelam, N. PEG-400 mediated an efficient eco-friendly synthesis of new isoxazolyl pyrido [2, 3-d] pyrimidines and their anti-inflammatory and analgesic activity. *Synthetic Communications*, 1-12 (2020).

27 Shamroukh, A., Rashad, A. & Abdelmegeid, F. The chemistry of pyrido [2, 3-d] pyrimidines and their applications. *Journal of Chemical and Pharmaceutical Research***8**, 734-772 (2016).

28 Rezazadeh, N. H., Buazar, F. & Matroodi, S. Synergistic effects of combinatorial chitosan and polyphenol biomolecules on enhanced antibacterial activity of biofunctionalaized silver nanoparticles. *Scientific Reports***10**, 1-13 (2020).

29 Romney, D. K., Arnold, F. H., Lipshutz, B. H. & Li, C.-J. Chemistry takes a bath: reactions in aqueous media. *The Journal of Organic Chemistry***83**, 7319–7322 (2018).

30 Olajire, A. & Mohammed, A. Green synthesis of nickel oxide nanoparticles and studies of their photocatalytic activity in degradation of polyethylene films. *Advanced Powder Technology***31**, 211-218 (2020).

31 Srihasam, S., Thyagarajan, K., Korivi, M., Lebaka, V. R. & Mallem, S. P. R. Phytogenic generation of NiO nanoparticles using Stevia leaf extract and evaluation of their in-vitro antioxidant and antimicrobial properties. *Biomolecules***10**, 89 (2020).

32 Khan, A. *et al.* Effect of Bi contents on key physical properties of NiO NPs synthesized by flash combustion process and their cytotoxicity studies for biomedical applications. *Ceramics International* (2020).

33 Diallo, A. *et al.* Structural, optical and photocatalytic applications of biosynthesized NiO nanocrystals. *Green Chemistry Letters and Reviews***11**, 166-175 (2018).

34 Ferreira, T. & Rasband, W. ImageJ user guide. *ImageJ/Fiji***1**, 155-161 (2012).

35 Buazar, F., Sweidi, S., Badri, M. & Kroushawi, F. Biofabrication of highly pure copper oxide nanoparticles using wheat seed extract and their catalytic activity: A mechanistic approach. *Green Processing and Synthesis***8**, 691-702 (2019).

36 Sabouri, Z. *et al.* Plant-based synthesis of NiO nanoparticles using salvia macrosiphon Boiss extract and examination of their water treatment. *Rare Metals*, 1-11 (2019).

37 Madhu, G., Maniammal, K. & Biju, V. Defect induced ferromagnetic interaction in nanostructured nickel oxide with core–shell magnetic structure: the role of Ni 2+ and O 2− vacancies. *Physical Chemistry Chemical Physics***18**, 12135-12148 (2016).

38 Kalaie, M. R., Youzbashi, A. A., Meshkot, M. A. & Hosseini-Nasab, F. Preparation and characterization of superparamagnetic nickel oxide particles by chemical route. *Applied Nanoscience***6**, 789-795 (2016).

39 Sayahi, M. H., Bahadorikhalili, S., Saghanezhad, S. J., Miller, M. A. & Mahdavi, M. Sulfonic acid-functionalized poly (4-styrenesulfonic acid) mesoporous graphene oxide hybrid for one-pot preparation of coumarin-based pyrido [2, 3-d] pyrimidine-dione derivatives. *Research on Chemical Intermediates***46**, 491-507 (2020).

40 Kobayashi, S. & Manabe, K. Green Lewis acid catalysis in organic synthesis. *Pure and applied chemistry***72**, 1373-1380 (2000).

41 Safaei-Ghomi, J. & Paymard-Samani, S. Facile and rapid synthesis of 5-substituted 1H-tetrazoles via a multicomponent domino reaction using nickel (II) oxide nanoparticles as catalyst. *Chemistry of Heterocyclic Compounds***50**, 1567-1574 (2015).

Figures

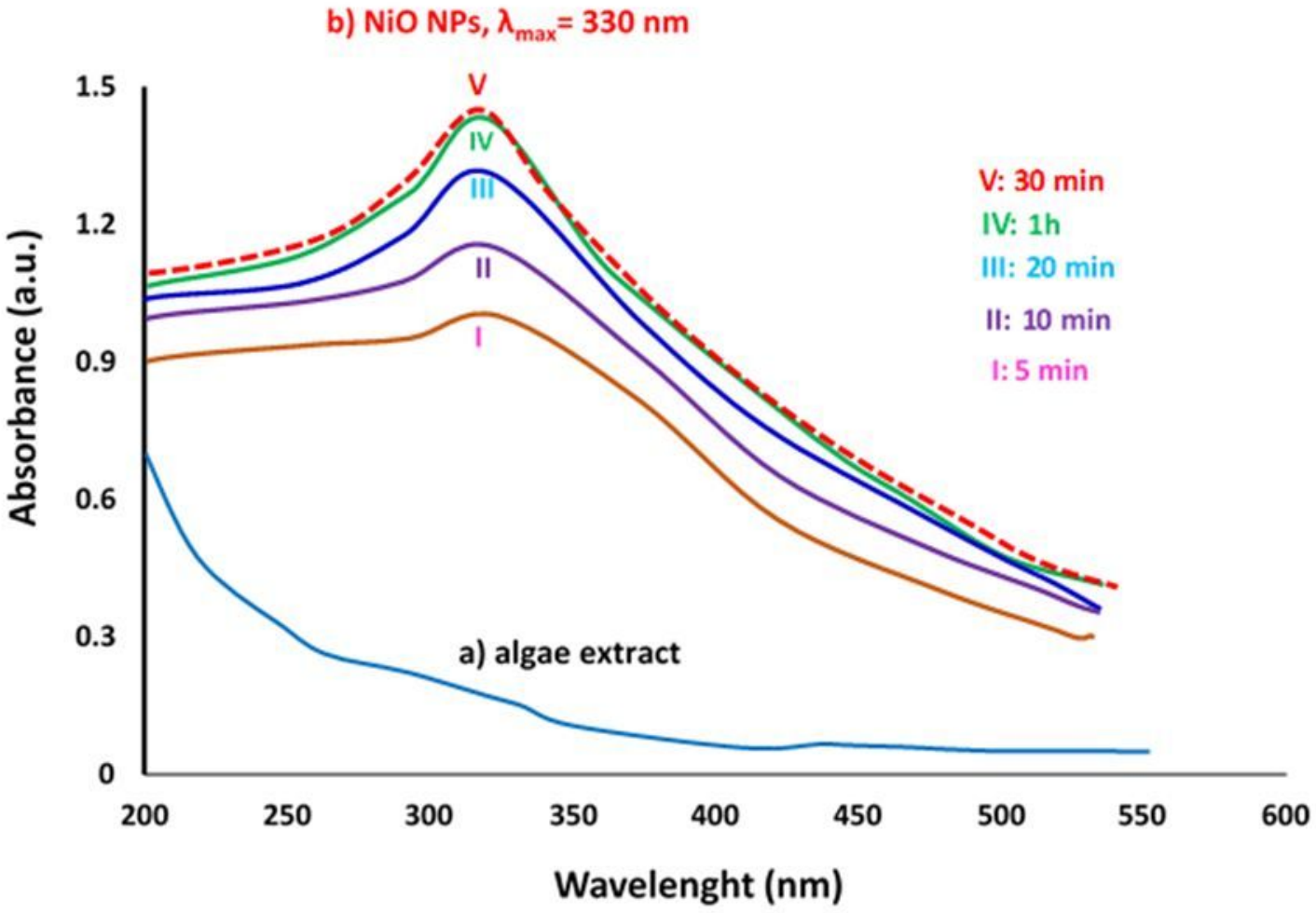

Figure 1

UV-visible spectra of (a) organic seaweed extract, (b) biogenic NiO NPs, as a function of time; inset images shows vivid color changes of reaction solution during the fabrication of NiO NPs.

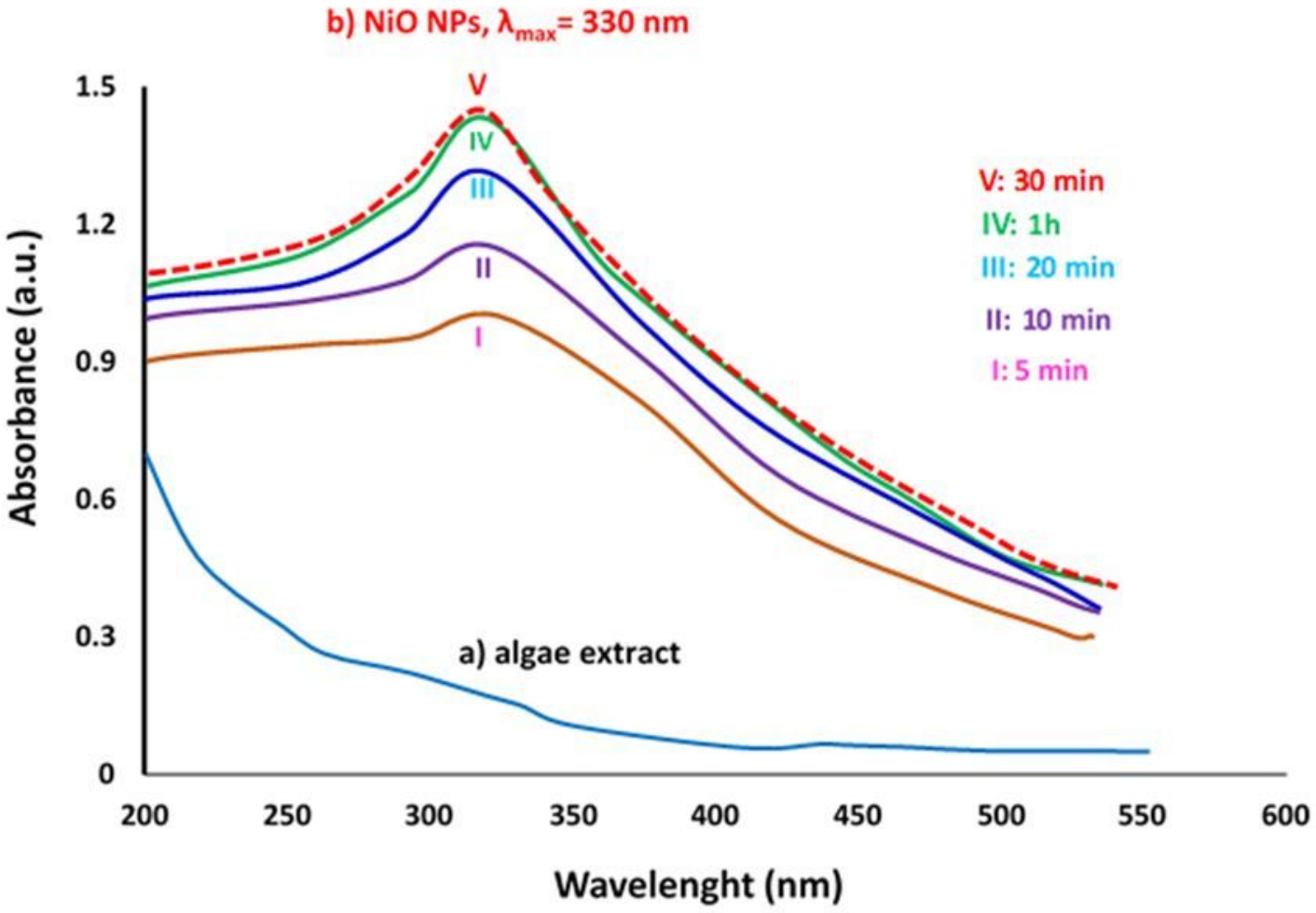

Figure 1

UV-visible spectra of (a) organic seaweed extract, (b) biogenic NiO NPs, as a function of time; inset images shows vivid color changes of reaction solution during the fabrication of NiO NPs.

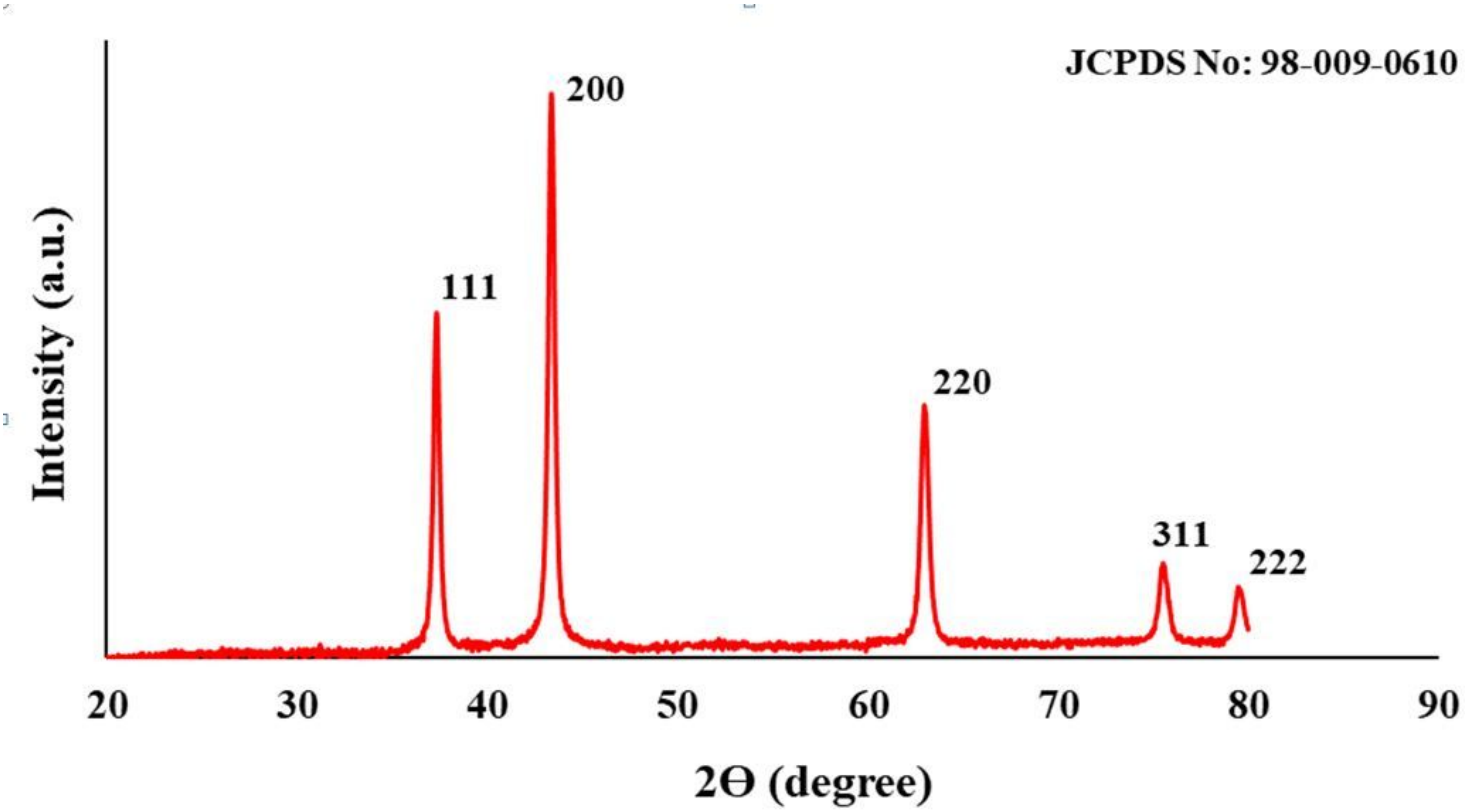

Figure 2

XRD pattern of biosynthesized NiO NPs using red marine algae extract

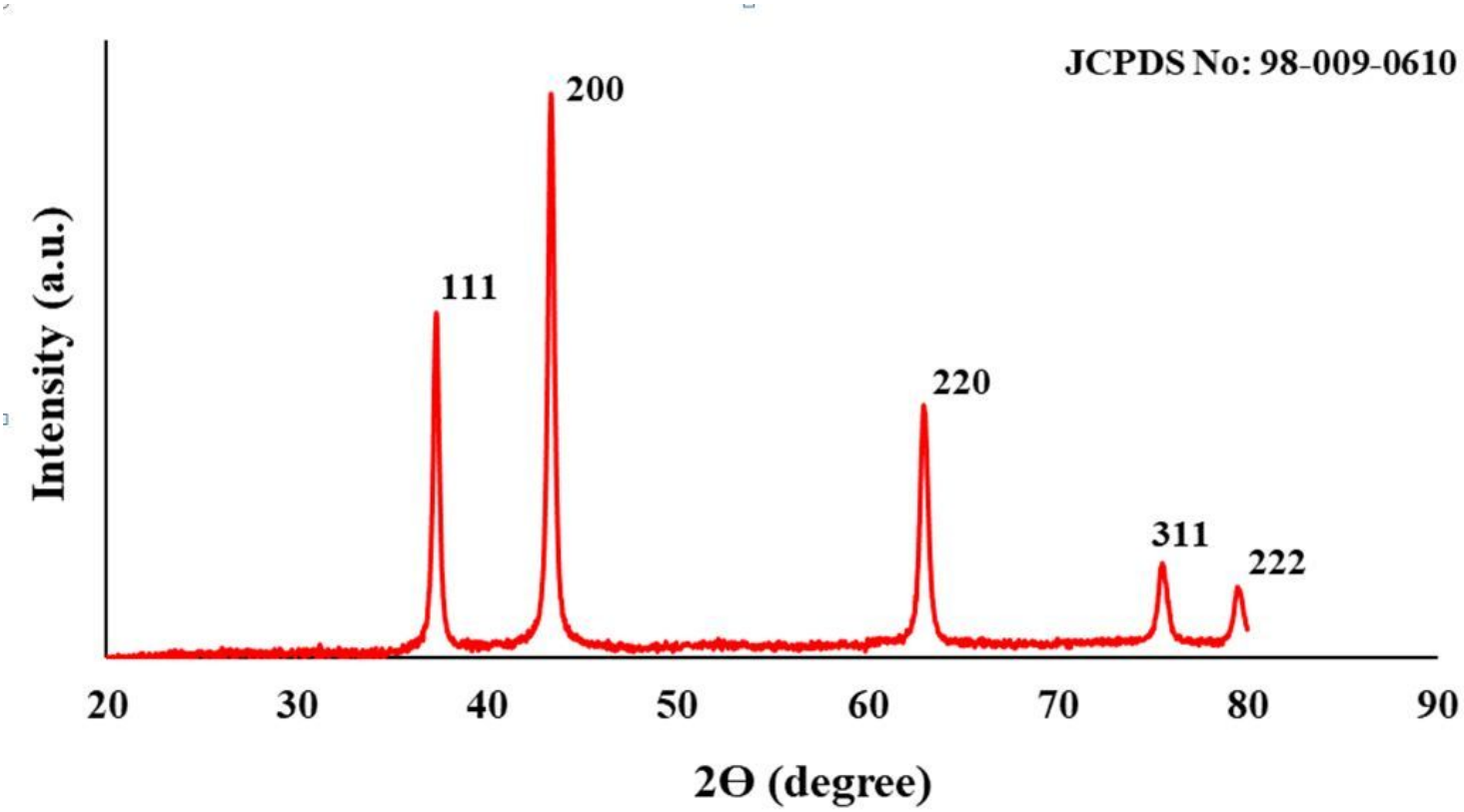

Figure 2

XRD pattern of biosynthesized NiO NPs using red marine algae extract

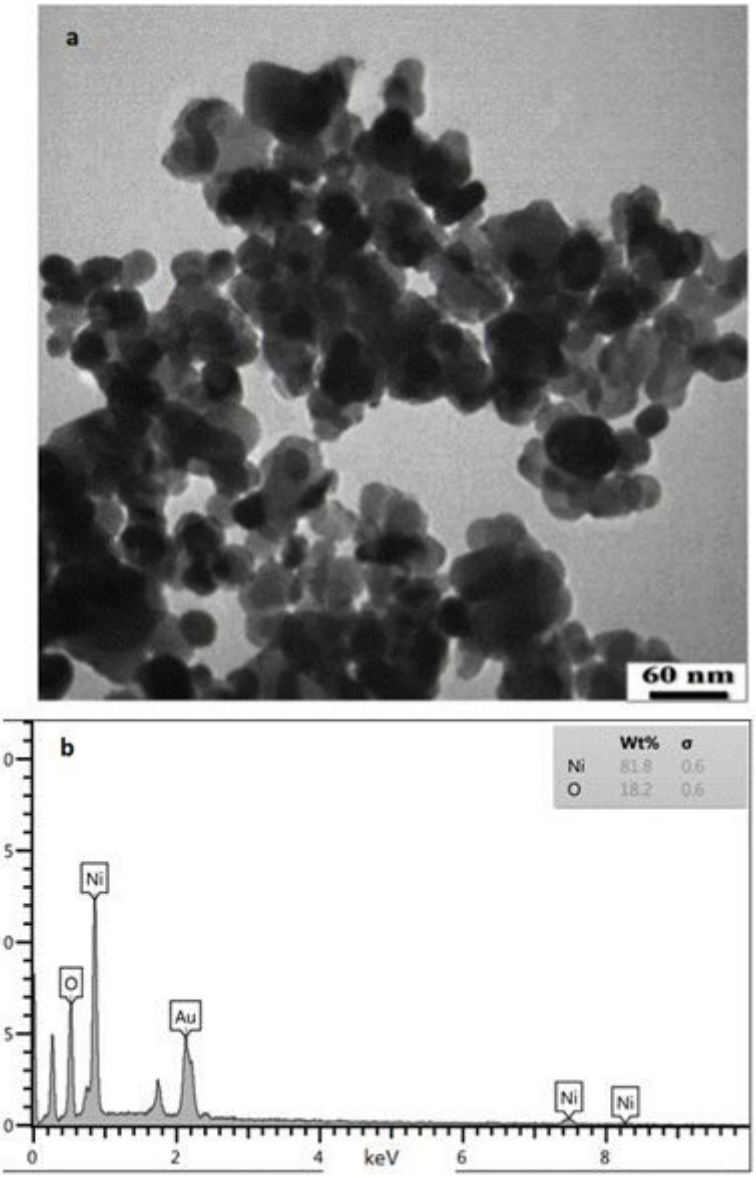

Figure 3

(a) The TEM image at 60.000 KX magnification and (b) EDX analysis of algal NiO NPs

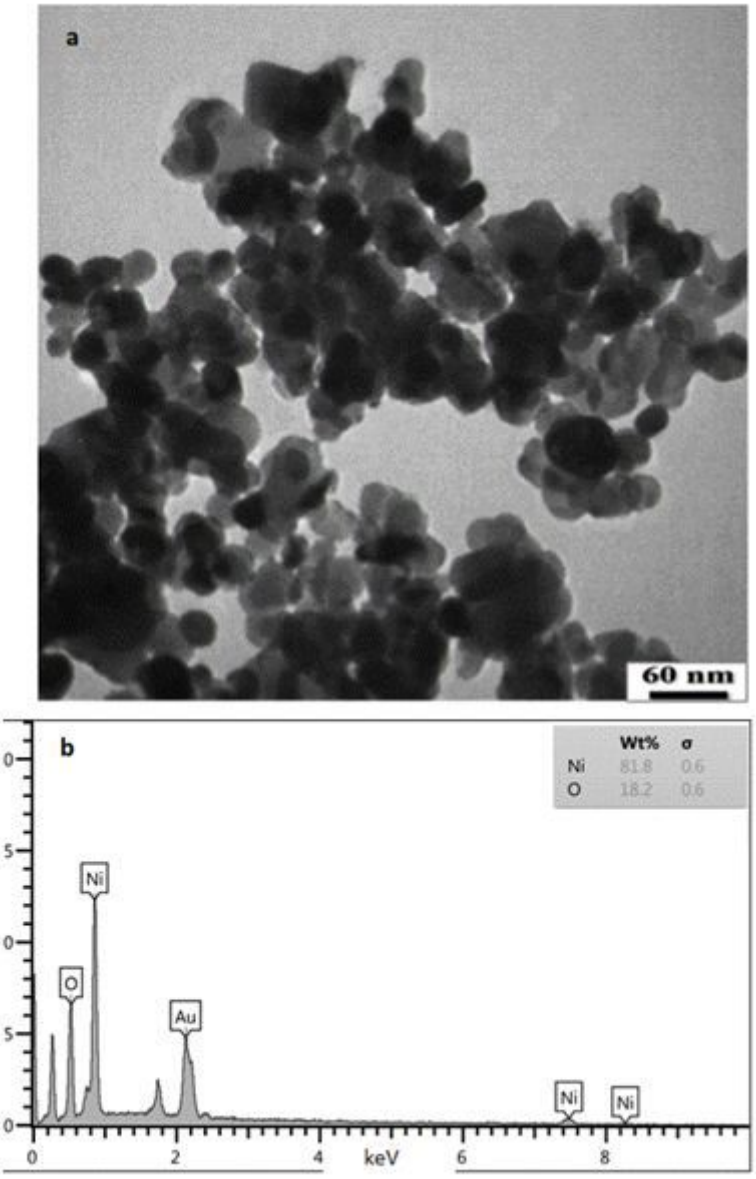

Figure 3

(a) The TEM image at 60.000 KX magnification and (b) EDX analysis of algal NiO NPs

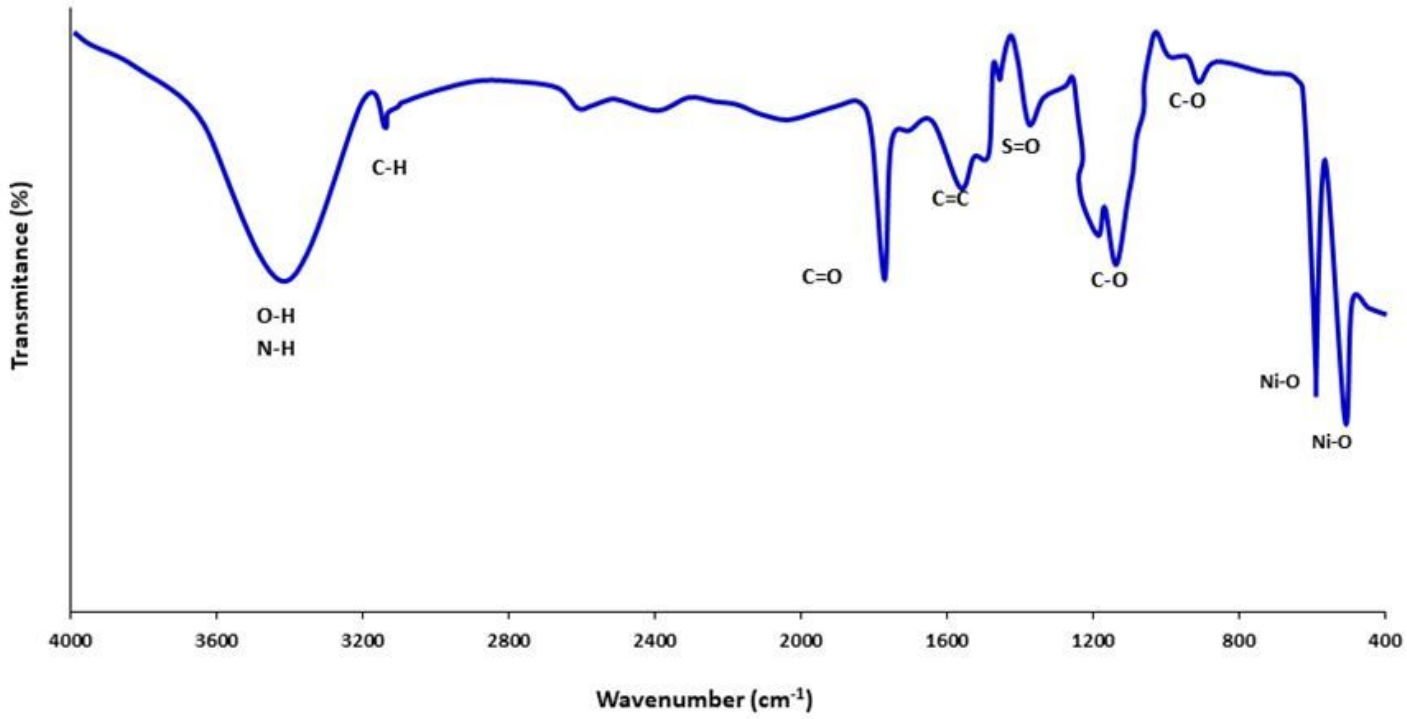

Figure 4

FTIR spectra of marine algae-mediated synthesized NiO NPs.

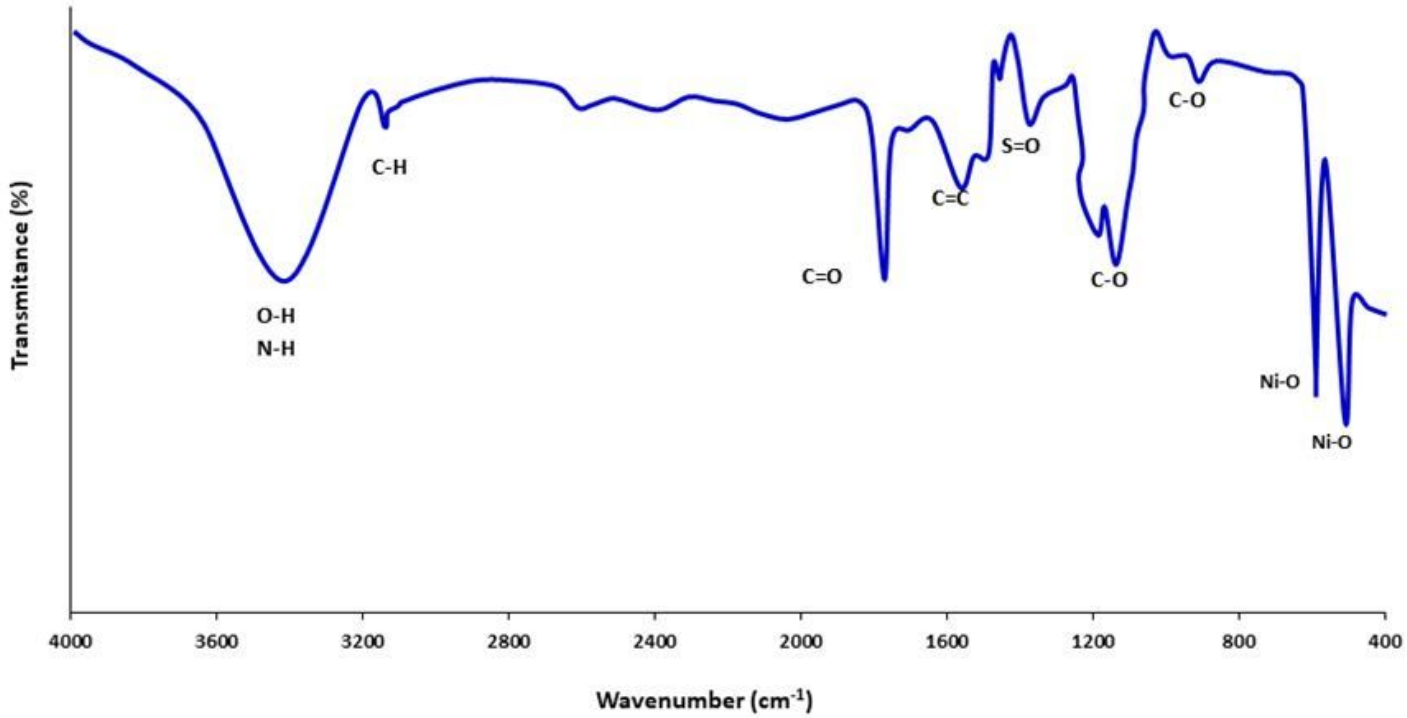

Figure 4

FTIR spectra of marine algae-mediated synthesized NiO NPs.

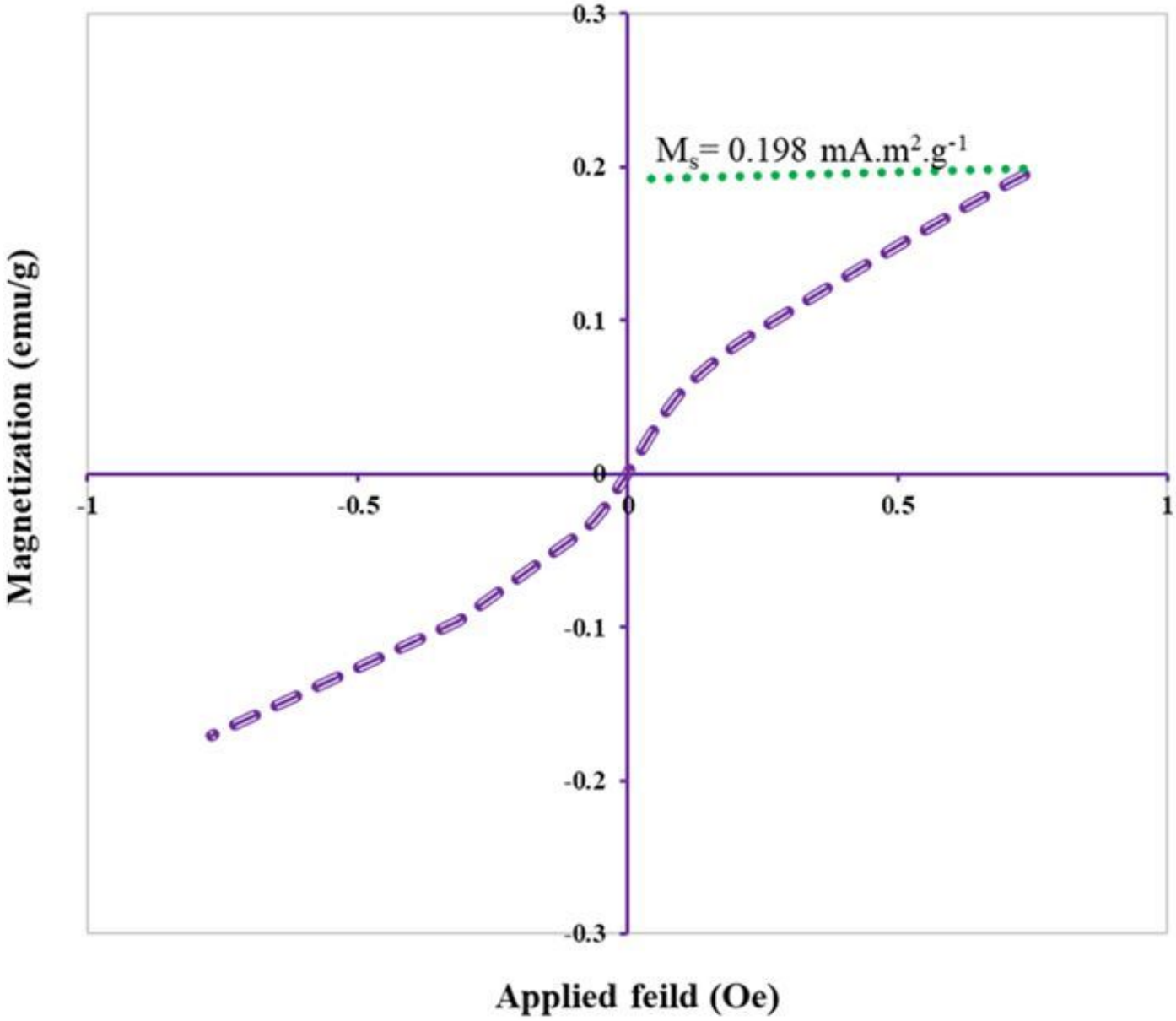

Figure 5

VSM magnetization curve of algal NiO NPs.

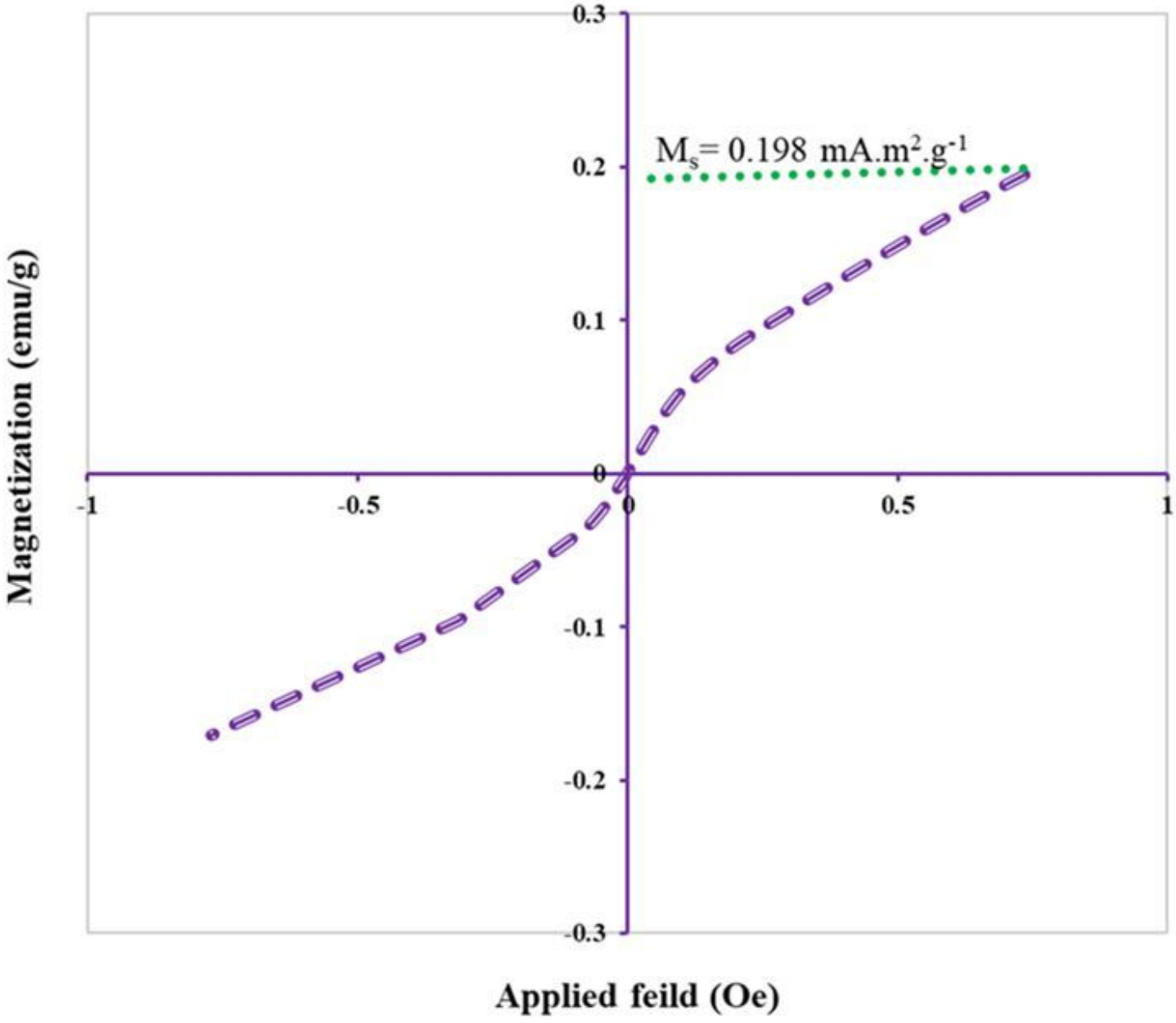

Figure 5

VSM magnetization curve of algal NiO NPs.

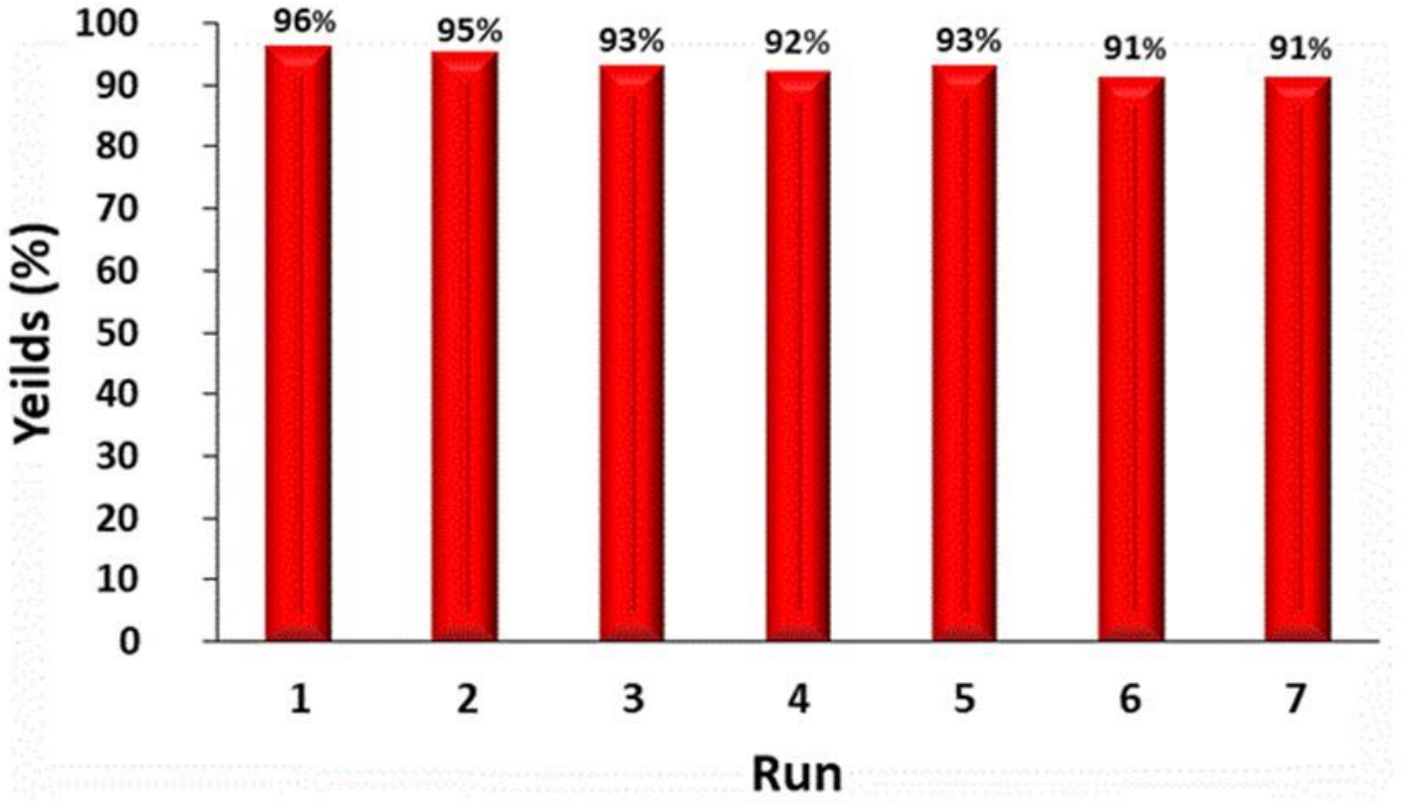

Figure 6

Reusability of algal NiO NPs catalyst in the synthesis of 5g in water

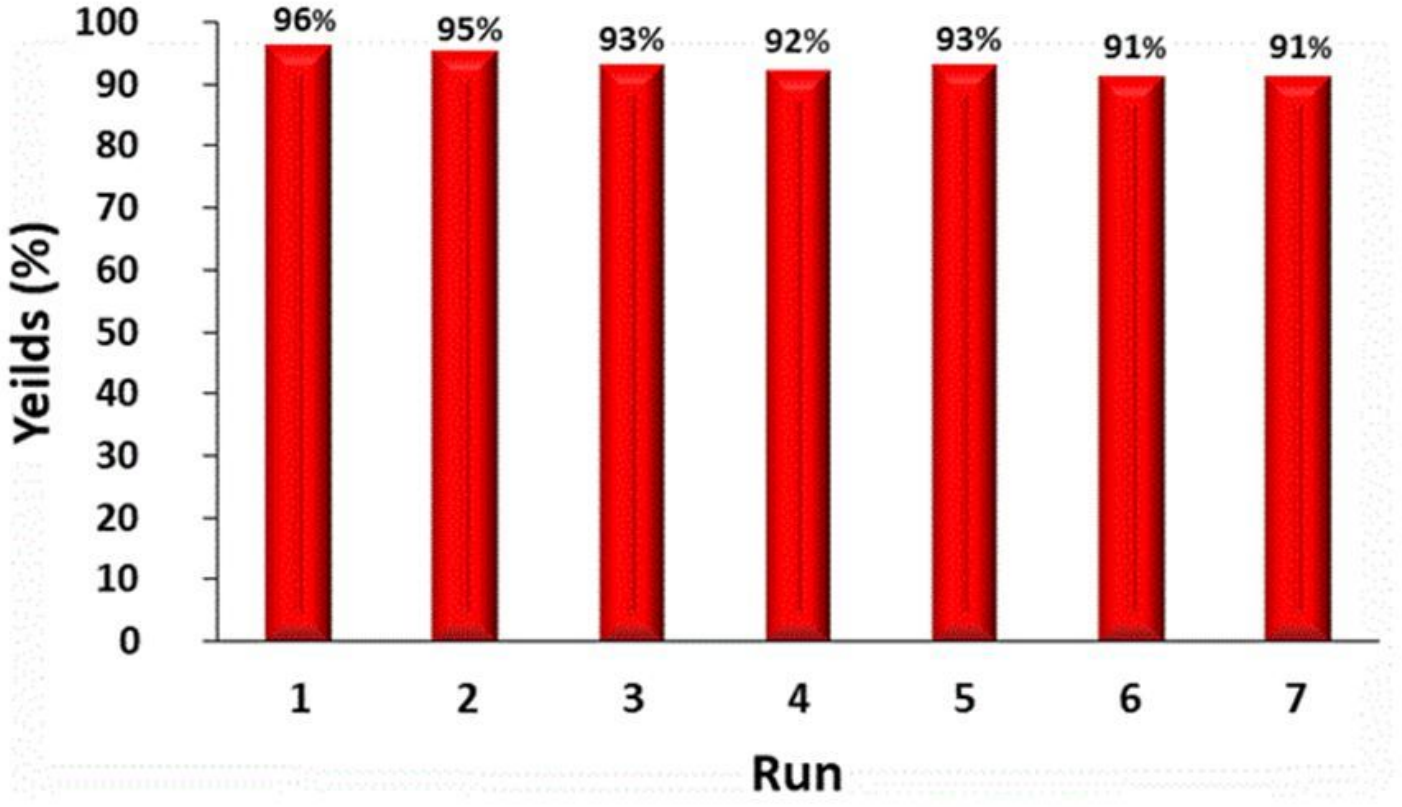

Figure 6

Reusability of algal NiO NPs catalyst in the synthesis of 5g in water

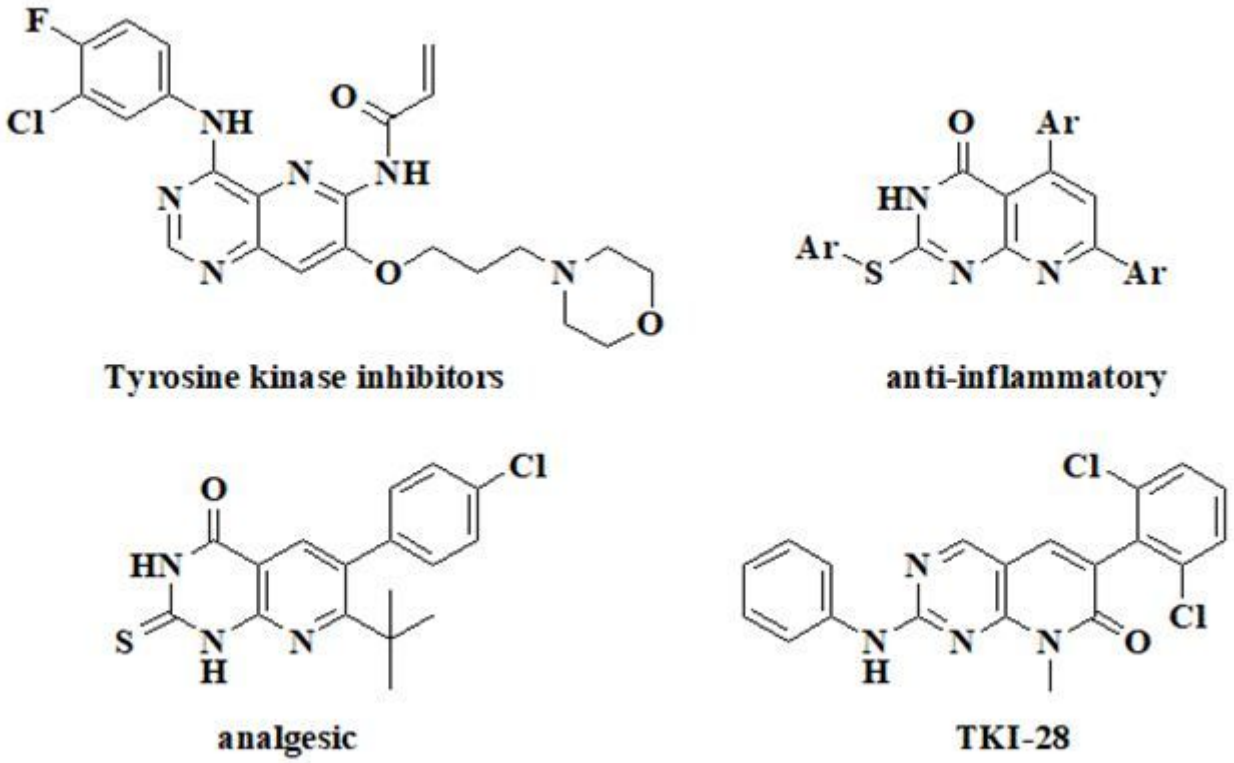

Figure 7

Selected pyridopyrimidine compounds with pharmaceutical properties27.

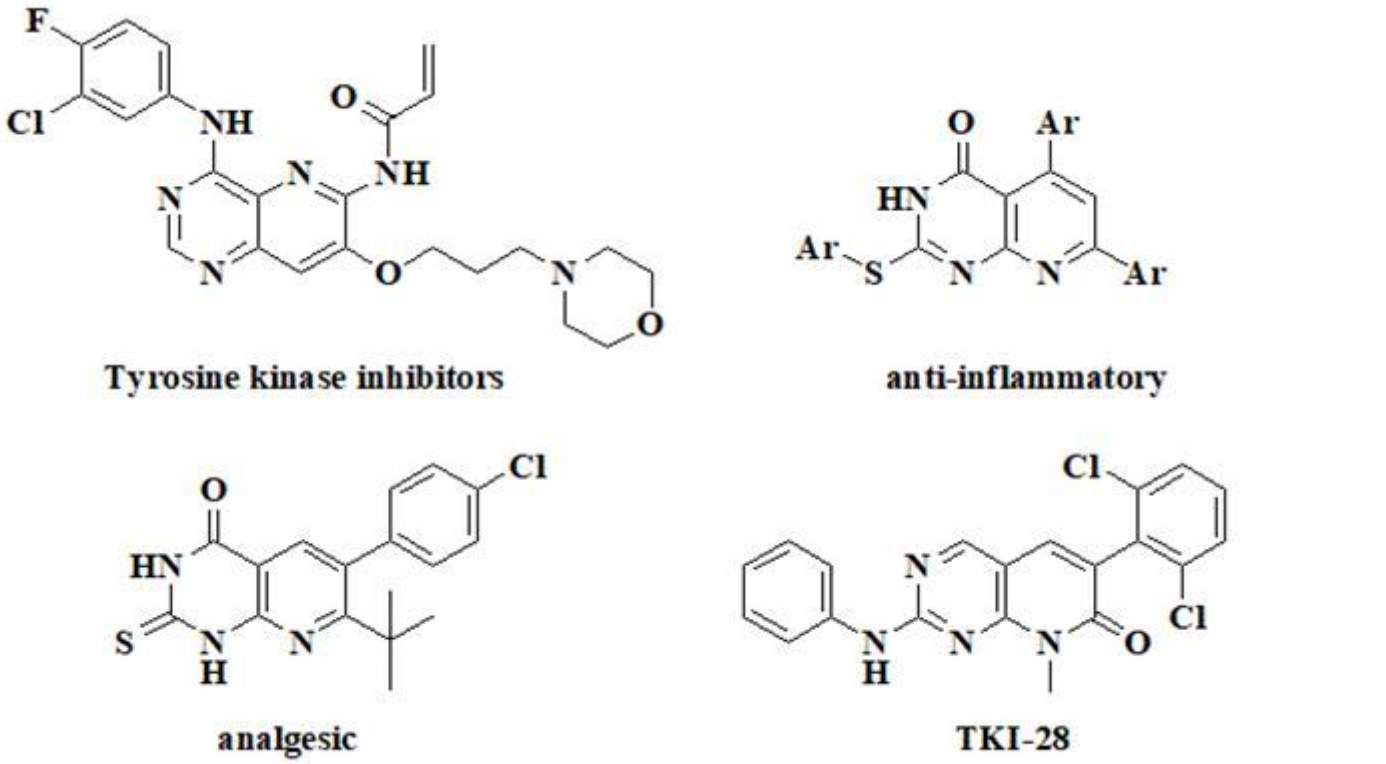

Figure 7

Selected pyridopyrimidine compounds with pharmaceutical properties27.

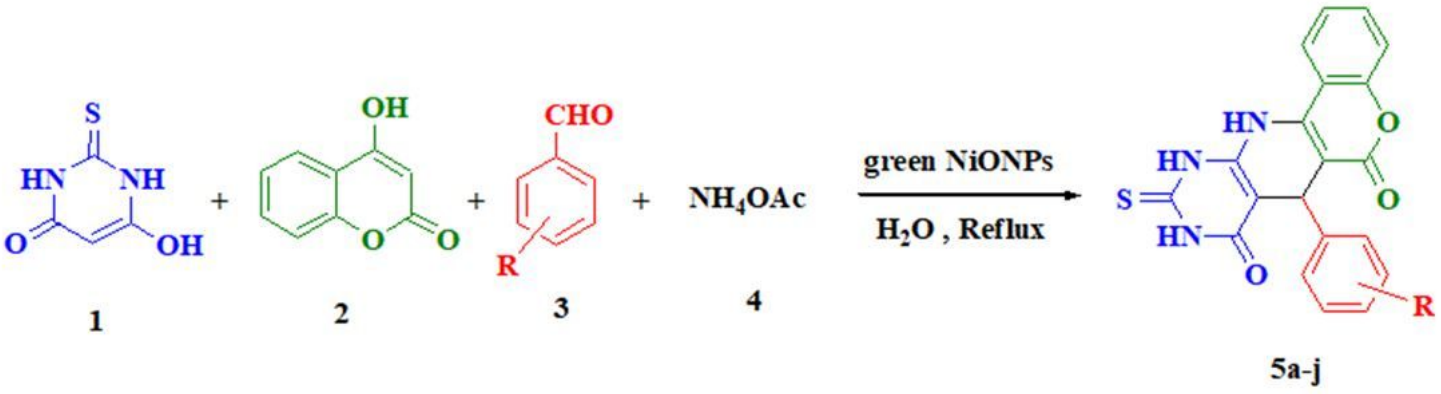

Figure 8

Synthesis of pyridopyrimidine derivatives 4a-j catalyzed by biogenic NiO NPs via a four-component reaction.

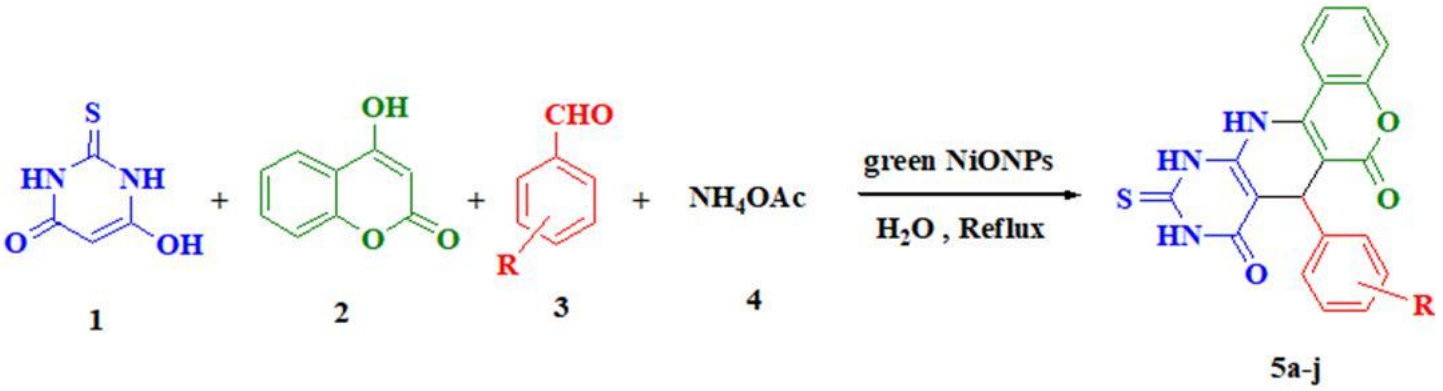

Figure 8

Synthesis of pyridopyrimidine derivatives 4a-j catalyzed by biogenic NiO NPs via a four-component reaction.

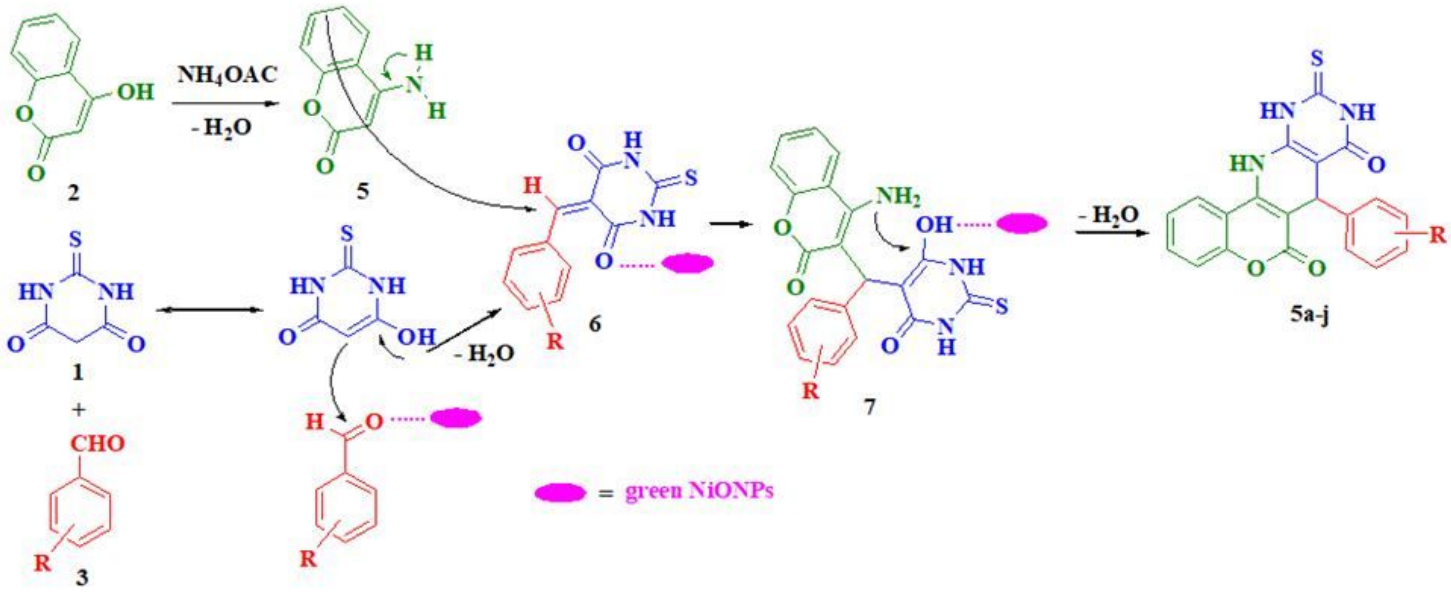

Figure 9

A proposed mechanism for the fabrication of pyridopyrimidine derivatives on the surface of biogenic NiO nanocatalyst.

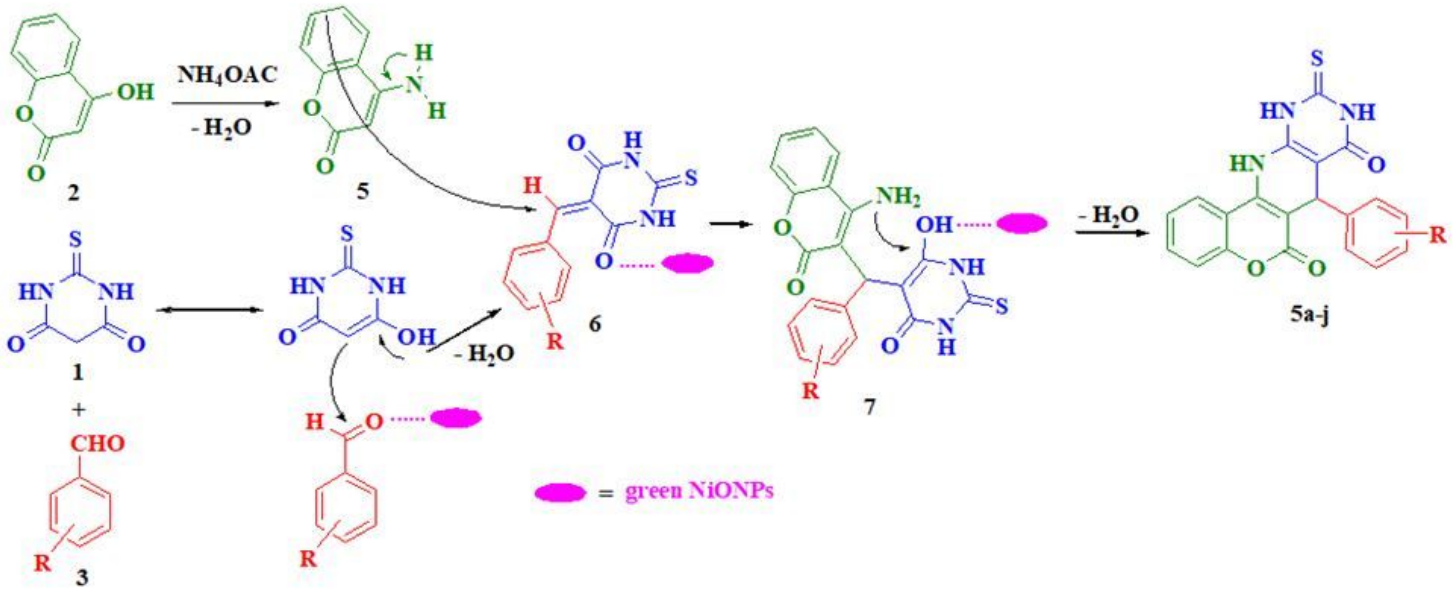

Figure 9

A proposed mechanism for the fabrication of pyridopyrimidine derivatives on the surface of biogenic NiO nanocatalyst.

Supplementary Files

This is a list of supplementary files associated with this preprint. Click to download.

- SupplementaryInformation.docx
- SupplementaryInformation.docx